7626 *J. Phys. Chem. A* **2005,** *109,* 7626−7635

Theoretical Isotropic Hyperfine Coupling Constants of Third-Row Nuclei (^{29}Si, ^{31}P, and ^{33}S)

L. Hermosilla, P. Calle, J. M. García de la Vega, and C. Sieiro*

Departamento de Química Física Aplicada, Facultad de Ciencias, Universidad Autónoma de Madrid, 28049 Madrid, Spain

Received: April 29, 2005

In a previous paper (Hermosilla, L.; Calle, P.; Garcia de la Vega, J. M.; Sieiro, C. *J. Phys. Chem. A* **2005**, *109*, 1114), an adequate computational protocol for the calculation of isotropic hyperfine coupling constants (hfcc's) was proposed. The main conclusion concerns the reliability of the scheme B3LYP/TZVP//B3LYP/6-31G* in the predictions of hfcc's with low computational cost. In the present study, we gain insight into the behavior of the above functional/basis set scheme on nuclei of the third row, for which few systematic studies have been carried out up to the present date. The systems studied are neutral, cationic, anionic, localized, and conjugated radicals, containing ^{29}Si, ^{31}P, and ^{33}S nuclei. After carrying out a regression analysis, we conclude that density functional theory (DFT) predictions on the hfcc's of the third-row nuclei are reliable for B3LYP/TZVP by using an optimized geometry with B3LYP/6-31G* combination. By comparison with other much more computationally demanding schemes, namely, B3LYP/cc-pVTZ and B3LYP/cc-pVQZ, we conclude that the B3LYP functional in conjunction with the TZVP basis set is the most useful computational protocol for the assignment of experimental hfcc's, not only for nuclei of first and second rows, but also for those of the third row.

Introduction

Radicals, very important molecular species involved in many processes of physical, chemical, and biological interest, can be studied with electron paramagnetic resonance (EPR) spectroscopy.[1] This technique measures the magnetic interactions between the unpaired electron and magnetic nuclei, which are represented by the hyperfine tensor. The factorization of this tensor gives rise to two terms: isotropic (Fermi term) and anisotropic (dipolar term). The isotropic term, the so-called hyperfine coupling constant, hfcc, is a function of the Fermi contact interaction of the unpaired electron with a determined nucleus and strongly depends on the spin density at the nucleus position.

The isotropic hyperfine coupling constant for a nucleus N, $a_{\mathrm{iso}}(N)$, is given by

$$a_{\mathrm{iso}}(N) = \frac{\mu_{\mathrm{o}}}{3}\, g_{\mathrm{e}} g_{\mathrm{N}} \beta_e \beta_N \langle S_z \rangle^{-1}\, \rho(N) \qquad (1)$$

where μ_{o} is the permeability of vacuum, g_{e} and g_{N} are the corresponding electronic and nuclear g factors, β_e is the Bohr magneton, β_N is the nuclear magneton of nucleus N, $\langle S_z \rangle$ is the mean value of S_z in the current electronic state, and $\rho(N)$ is the Fermi contact integral for nucleus N, whose value is given by the expression

$$\rho(N) = \sum_{\mu\nu} P^{\alpha\beta}_{\mu\nu} \langle \phi_\mu(r_{kN}) | \delta(r_{kN}) | \phi_\nu(r_{kN}) \rangle \qquad (2)$$

$P^{\alpha\beta}_{\mu\nu}$ is an element of the one-electron spin density matrix, ϕ denotes the atomic basis functions, and δ is the Dirac delta operator.

As is well-known, the isotropic term, which has received great attention from theoretical chemists and physics, is much more difficult to compute in quantitative agreement with the experimental data than the corresponding anisotropic term. This is due to the fact that this property is very sensitive to the quality of the wave function employed and the level of calculation used, since the hfcc depends on the electron correlation, one-electron basis set, and the use of very adequate molecular geometry.

Many works have been done to obtain accurate values of hfcc's in the past.[2] Although top-level post-HF methods, e.g., multireference configuration interaction (MRCI), quadratic configuration interaction (QCI), and coupled cluster (CC) methods, are more accurate, they also require correlated wave functions and, hence, highly computationally demanding calculations. Recently, the use of methods based on density functional theory (DFT) for the calculation of radicals has been well-established, because DFT methods partly include electron correlation through the exchange-correlation functional, leading to accurate values of spin densities with considerably lower computational time. Their favorable scaling, as compared with correlated molecular orbital (MO) methods, allows us to obtain spin densities for much larger-sized radicals by using a much less expensive basis set. The performance of several hybrid DFT methods (B3LYP, B3P86, and B3PW91) with different basis sets (6-31G*, TZVP, EPR-III, and cc-PVQZ) has been previously studied for nuclei of the first and second rows.[3a,b]

To our knowledge, very few analyses have been carried out in the case of the third-row nuclei. Radicals containing the ^{31}P nucleus have received attention by Nguyen et al.[4,5] and Cramer et al.[6,7] These works are the biggest constituting analyses in the comparison of experimental and theoretical hyperfine data for this nucleus. In the first work, a set of 24 experimental $a_{\mathrm{iso}}(^{31}\mathrm{P})$ of small radicals containing phosphorus are compared with those calculated by using B3LYP and B3PW91 hybrid functionals with TZVP, TZVP′, TZVP″, and IGLO-III basis

---

* Correspondence author. Phone: +34-91-4974951. Fax: +34-91-4974512. E-mail: carlos.sieiro@uam.es.

10.1021/jp0522361 CCC: $30.25

sets and molecular geometry optimized with B3LYP or B3PW91/6-311G(d,p). The values obtained for the hfcc's of the ^{31}P nucleus are reasonably accurate. For the smaller phosphorus-containing radicals, Nguyen et al. carried out ab initio MO and DFT calculations in order to make a comparative investigation. They conclude that the use of either UMP2/6-311G(d,p) or QCISD/6-311G(d,p) geometries enhances the accuracy of B3LYP hfcc values considerably, but they can only be applied to small systems. In Cramer's work, the hfcc's of 25 phosphoranyl radicals containing 4 different nuclei, ^{1}H, ^{19}F, ^{31}P, and ^{35}Cl, were calculated at 3 levels of theory: UHF, PUHF, and MP2. Moreover, 20 a_{iso}(^{31}P) were compared with available experimental data. They conclude that the most accurate theoretical predictions were obtained from calculations at the MP2/6-311G**//UHF/6-31G** level. However, the spin contamination is not well-resolved in this kind of calculation.

For ^{33}S, to our knowledge, the most significant study that compares theoretical and experimental hfcc's was carried out by Kaszynski.[8] In this case, 13 a_{iso}(^{33}S), obtained by using the B3LYP hybrid functional with 6-31G(d) and cc-pVDZ basis sets, were compared with experimental data. Nevertheless, the calculated hfcc values are not explicitly given and are manipulated as a whole in a regression analysis.

For the ^{29}Si nucleus, no important study proposing a computational protocol to obtain hfcc's has been carried out up to the present date. Only in scarce papers is it possible to find theoretical values of hfcc's for either some specific radical or small groups of radicals containing silicon.

In our previous paper,[3a] 18 hfcc values for the 7 nuclei of the third row were studied. The regression analysis for these nuclei is less significant than the rest of the studied nuclei because of the small number of computed hfcc's. The aim of this paper is to fill this gap by investigating the reliability of DFT methodology to predict, with a certain degree of accuracy, the isotropic hyperfine coupling constants of radicals containing nuclei of the third row: ^{29}Si, ^{31}P, or ^{33}S. This goal will basically be performed using a statistical analysis by comparing the calculated and experimental hfcc's. At the present, the amount of available experimental data for the rest of the third-row nuclei (^{23}Na, ^{25}Mg, ^{27}Al, and ^{35}Cl) is not sufficient to carry out a reliable regression analysis.

Computational Details

We have considered a set of 75 paramagnetic species contain at least one ^{29}Si ($I = {}^{1}/_{2}$), ^{31}P ($I = {}^{1}/_{2}$) or ^{33}S ($I = {}^{3}/_{2}$) nuclei and whose experimental hfcc's were well-known. The studied set comprises neutral, cationic, anionic, localized, and conjugated radicals. In the present study, hfcc's of the radicals studied were calculated by using the B3LYP hybrid functional[9a,b] with three different basis sets, TZVP,[10] cc-pVTZ, and cc-pVQZ.[11] The first one is a DFT-optimized valence triple-ζ basis, whereas the other two are Dunning's correlation consistent polarized valence triple- and quadruple-ζ basis sets, respectively.

In this investigation, the geometrical optimization was carried out by using the B3LYP/6-31G* scheme because of its low computational cost for the very large radicals analyzed here. Although geometry plays an important role in the calculation of hfcc's, the selected radicals present, in general, well-defined geometries for their ground states. The geometries of the selected radicals are depicted in Figures 1, 2, and 3, and show the 25 radicals containing ^{29}Si, ^{31}P, and ^{33}S nuclei, respectively, which are ordered by molecular size. Because of the high variety of the studied radicals, their ordering can be performed using many logical criteria, but the molecular size criterion was finally adopted as the most simple and easiest to use. Molecular geometries were fully optimized at the B3LYP level employing the 6-31G* basis set in order to maintain the same criteria used in ref 3. In the case of methyl group presence, the experimental equivalence of the methyl protons implies their rapid rotation. Thus, by averaging the three ^{1}H hfcc's for the theoretical equilibrium structure, a fair estimate of rotationally averaged values is obtained. This behavior is accomplished for other freely rotating groups (CF_3, CCl_3, ...). On the other hand, the average of the hfcc's has been carried out for radical-containing magnetically equivalent nuclei. The effects of vibrational average on the calculated hfcc's have not been considered in this study. The majority of these radicals are very large, and hence, the incremental increase in the computational cost does not justify its inclusion.

A total of 206 hfcc's have been analyzed, of which 98 correspond to ^{1}H, 25 to nuclei of the second row, 77 to ^{29}Si, ^{31}P, and ^{33}S nuclei, and 6 to the ^{35}Cl nucleus. All computations were performed using the spin-unrestricted theory of *Gaussian 03*.[12]

Results and Discussion

Isotropic Hyperfine Coupling Constants. The calculated and experimental hfcc's in gauss are summarized in Tables 1−3. All these tables have 10 columns: The first one indicates the number of the radical, the second one corresponds to the empirical formulas, and the third and fourth contain the symmetry of the electronic ground state and its total energy at the B3LYP/TZVP//B3LYP/6-31G* level, respectively (in parentheses, B3LYP/cc-pVD(T or Q)Z//B3LYP/6-31G* energies). In the fifth one, the nuclei with their isotopic masses appear. In this column and for each radical, the nuclei of the third row are presented in the first place. To identify the nuclei unequivocally, additional information is included. The following three columns report the theoretical hfcc values obtained with the schemes: (A) B3LYP/TZVP//B3LYP/6-31G*, (B) B3LYP/(cc-pVQZ or cc-pVTZ)//B3LYP/6-31G*, and (C) other post-HF calculations. We have included a highly demanding computational calculation (B), to compare the simpler proposed scheme (A) with other much more sophisticated schemes. In the last two columns, the experimental hfcc's and their references are summarized. As is well-known, the sign of a_{iso} is not determined when an experimental EPR spectrum is analyzed. The corresponding sign is assigned on the basis of the theoretical results. Thus, the absolute values for the experimental data are given.

The main aim of this paper is to provide a useful computational protocol to the EPR spectroscopists for a theoretical prediction of the hfcc values, allowing a correct assignment of the experimental data. However, some interesting general behavior obtained in the present calculations will be commented on here, but not in depth for each radical.

In this paper, only the theoretical data for which experimental values are available in the literature have been considered. For those nuclei without experimental values, those calculated here are disposable on the request to the authors.

Silicon Radicals. The silyl radicals (**1a**−**9a**, **19a**−**20a**) have a pyramidal conformation at the silicon spin-bearing atoms, ^{29}Si$_{\alpha}$, in contrast to the planarity of alkyl radicals. The values of X−Si−Y angles (X and Y are H, F, C, N, O, Si, or Cl) obtained in this work agree with the results previously obtained by Apeloig et al.[13] for large series of polysilyl radicals. Because of a stronger s−p spin polarization effect, the values of a_{iso}(^{29}Si$_{\alpha}$) (−63 to −457 G) are larger than those of a_{iso}(^{13}C$_{\alpha}$) for the corresponding alkyl radicals. However, for protons, the a_{iso}-

TABLE 1: Theoretical Hyperfine Coupling Constants (G) of Radicals Containing ^{29}Si Nuclei at (A) B3LYP/TZVP//B3LYP/6-31G* and (B) B3LYP/cc-pVQZ[a] (or cc-pVTZ[b])//B3LYP/6-31G* Levels.[c] (C) Other Theoretical Results

					a_{iso} (theoretical)			experimental	
no.	radical	state	energy (au)	nuclei	A	B	C	a_{iso}	ref
1a	$SiF_3^{\bullet}$ [d]	$^2A_1$	−589.291312	^{29}Si	−457.1	−456.9[a]	−501.9[cc]	498.0	(35)
			(−589.348733)	$3\ ^{19}F$	126.5	118.3	129.2	136.6	
2a	$SiCl_3^{\bullet}$ [e]	$^2A_1$	−1670.278915	^{29}Si	−391.8	−404.0[a]	−416.1[cc]	416.0	(36)
			(−1670.350540)	$3\ ^{35}Cl$	11.3	11.2	11.3	12.4	
3a	$CH_5Si^{\bullet}$ [f]	^2A	−330.597612	^{29}Si	−162.7	−161.4[a]	−184.2[dd]	181.0	(37)
			(−330.616173)	$3\ ^{1}H$	8.3	8.3		8.0	(38)
				$2\ ^{1}H$	14.4	15.6	6.0	11.8	
4a	$CH_3SiCl_2^{\bullet}$ [g]	$^2A'$	−1249.953225	^{29}Si	−275.7	−280.7[a]	−301.9[ee]	295	(36)
			(−1250.008828)	$2\ ^{35}Cl$	9.2	8.9		10.5	
5a	$C_2H_7Si^{\bullet}$ [h]	^2A	−369.938776	^{29}Si	−161.3	−160.2[a]	−185.5[dd]	183.0	(38−40)
			(−369.961907)	^{1}H	18.2	19.6	10.3	17.0	
				$6\ ^{1}H$	7.5	7.4		7.2	
6a	$C_3H_9Si^{\bullet}$ [i]	$^2A'$	−409.280033	^{29}Si	−159.8	−158.7[a]	−189.8[cc]	181.0	(37−40)
			(−409.307624)	$9\ ^{1}H$	6.5	6.5	5.5	6.3	
7a	$C_3H_9O_3Si^{\bullet}$ [j]	^2A	−635.100522	^{29}Si	−303.0	−305.8[a]	*ff*	339.0	(41)
			(−635.161722)						
8a	$C_6H_{15}Si^{\bullet}$ [k]	^2A	−527.245908	^{29}Si	−145.5	−144.1[a]	*ff*	170.0	(39−40)
			(−527.286041)	$6\ ^{1}H$	7.8	7.8		5.7	
				$9\ ^{1}H$	−0.2	−0.2		0.2	
9a	$C_5H_{15}Si_2^{\bullet}$ [l]	$^2A'$	−778.683613	^{29}Si	−121.1	−125.3[a]	−147.9[ee]	137.0	(39)
			(−778.708421)	$6\ ^{1}H$	8.0	7.9		8.2	
				$9\ ^{1}H$	0.5	0.4		0.5	
10a	$C_9H_{14}Si^{\bullet-}$ [m]	$^2A''$	−641.031134	^{29}Si	5.3	6.4[b]	*ff*	5.2	(42)
			(−641.051317)	$^{1}H_{2,6}$	−3.4	−3.2		2.7	
				$^{1}H_{3,5}$	−0.3	−0.2		1.1	
				$^{1}H_{4}$	−10.0	−9.8		8.1	
				$9\ ^{1}H$	0.4	0.4		0.3	
11a	$C_9H_{12}O_2Si^{\bullet-}$ [n]	$^2A''$	−790.406400	^{29}Si	1.5	1.6[b]	*ff*	1.5	(43)
			(−790.425508)	$^{1}H_{3}$	−3.1	−2.9		2.7	
				$^{1}H_{5}$	−2.1	−1.9		2.1	
				$^{1}H_{6}$	−2.1	−2.0		2.5	
12a	$C_6H_{18}N_2Si_2^{\bullet-}$ [o]	^2B_g	−928.209265	$2\ ^{29}Si$	6.8	7.5[b]	*ff*	7.0	(44)
			(−928.238510)	$2\ ^{14}N$	5.0	3.5		6.3	
13a	$C_8H_{20}Si_2^{\bullet-}$ [p]	^2B_g	−896.057267	$2\ ^{29}Si$	6.6	7.9[b]	*ff*	6.7	(42)
			(−896.086889)	$^{1}H_{1,2}$	−8.2	−7.8		7.5	
				$18\ ^{1}H$	0.3	0.3		0.4	
				$^{13}C_{1,2}$	3.4	−0.5		5.6	
14a	$C_{10}H_{22}Si_2^{\bullet-}$ [q]	^2A_u	−973.511397	$2\ ^{29}Si$	6.1	6.6[b]	*ff*	5.7	(42)
			(−973.573556)	$^{1}H_{1,4}$	−6.6	−6.3		6.7	
				$^{1}H_{2,3}$	-3.2	−2.7		3.2	
				$18\ ^{1}H$	0.3	0.3		0.2	
15a	$C_{12}H_{20}O_2Si_2^{\bullet-}$ [r]	^2B_g	−1199.142848	$2\ ^{29}Si$	1.3	1.2[b]	*ff*	1.5	(43)
			(−1199.176348)	$^{1}H_{3,6}$	−2.9	−2.7		2.8	
16a	$C_{12}H_{22}Si_2^{\bullet-}$ [s]	^2A	−1049.735404	$2\ ^{29}Si$	5.0	5.8[b]	*ff*	4.5	(42)
			(−1049.770741)	$^{1}H_{3,6}$	0.8	0.8		0.5	
				$^{1}H_{4,5}$	−5.9	−5.7		5.2	
				$18\ ^{1}H$	0.3	0.3		0.2	
17a	$C_{12}H_{22}Si_2^{\bullet-}$ [t]	^2A_u	−1049.757632	$2\ ^{29}Si$	5.8	6.7[b]	*ff*	6.2	(42, 45)
			(−1049.793106)	$18\ ^{1}H$	0.3	0.3		0.3	
				$^{1}H_{2,3,5,6}$	-1.9	−1.8		1.8	
18a	$C_{12}H_{22}N_2Si_2^{\bullet-}$ [u]	$^2A_2$	−1159.391279	$2\ ^{29}Si$	4.2	4.2[b]	*ff*	3.9	(43, 46)
			(−1159.431871)	$2\ ^{14}N$	3.1	5.0		4.0	
				$^{1}H_{2,3,5,6}$	−1.9	−1.8		2.0	
19a	$C_{12}H_{27}Si^{\bullet}$ [v]	$^2A_1$	−763.069915	^{29}Si	−140.4	−143.0[b]	*ff*	163.0	(47)
			(−763.192469)						
20a	$C_9H_{27}Si_4^{\bullet}$ [w]	$^2A_1$	−1517.499457	^{29}Si	−62.8	−63.3[b]	−73.2[ee]	64.0	(39, 40, 48)
			(−1517.548128)	$3\ ^{29}Si$	4.0	3.4		7.1	
				$27\ ^{1}H$	0.4	0.4		0.4	
21a	$C_{16}H_{24}Si_2^{\bullet-}$ [x]	$^2B_1$	−1203.492267	$2\ ^{29}Si$	5.2	5.4[b]	*ff*	4.6	(42)
			(−1203.529447)	$^{1}H_{2,3}$	−2.3	−2.2		2.3	
				$^{1}H_{5,8}$	−3.4	−3.1		3.2	
				$^{1}H_{6,7}$	−1.2	−1.2		1.4	
22a	$C_{16}H_{24}Si_2^{\bullet-}$ [y]	^2B_g	−1203.490579	$2\ ^{29}Si$	3.9	4.0[b]	*ff*	3.5	(42)
			(−1203.527615)	$^{1}H_{2,6}$	−1.9	−1.9		2.1	
				$^{1}H_{3,7}$	−1.6	−1.6		1.7	
				$^{1}H_{4,8}$	−5.2	−4.9		4.7	
23a	$C_{16}H_{24}Si_2^{\bullet-}$ [z]	^2B_g	−1203.495733	$2\ ^{29}Si$	2.9	3.3[b]	*ff*	2.7	(42)
			(−1203.536173)	$^{1}H_{1,5}$	−4.8	−4.6		4.6	
				$^{1}H_{3,7}$	0.7	0.7		0.2	
				$^{1}H_{4,8}$	−4.8	−4.5		4.5	

TABLE 1: (Continued)

no.	radical	state	energy (au)	nuclei	a_{iso} (theoretical) A	B	C	experimental a_{iso}	ref
24a	$C_{18}H_{40}Si_4^{\bullet+}$ [aa]	^2A	−1868.200356 (−1868.263939)	$4^{29}Si$ $4^1H_{1,2,4,5}$ 36^1H	−18.7 −2.8 0.3	−19.1[b] −2.6 0.3	[ff]	20.9 3.0 0.2	(49)
25a	$C_{18}H_{44}Si_4^{\bullet+}$ [bb]	$^2B_3$	−1870.652958 (−1870.718517)	$4^{29}Si$ 4^1H_β $4^1H_\beta'$ 36^1H	−9.8 8.3 7.2 0.4	−10.0[b] 8.3 7.1 0.4	[ff]	12.5 8.6 7.3 0.3	(49)

[a] (B3LYP/cc-pVQZ//B3LYP/6-31G*). [b] (B3LYP/cc-pVTZ//B3LYP/6-31G*). [c] The corresponding energies are shown in parentheses. [d] Trifluor silyl. [e] Trichloro silyl. [f] Methyl silyl. [g] Dichloromethyl silyl. [h] Dimethyl silyl. [i] Trimethyl silyl. [j] Trimetoxi silyl. [k] Triethyl silyl. [l] Trimethylsilyldimethyl silyl. [m] Trimethylsilylbenzene anion. [n] 2-trimethylsilyl-*p*-benzoquinone anion. [o] Bis(trimethylsilyl)diimine anion. [p] Trans-1,2-bis(trimethylsilyl)ethene anion. [q] (*E*-*E*)-1,4-Bis(trimethylsilyl)-buta-1,3-diene anion. [r] 2,5-Bis(trimethylsilyl)-*p*-benzoquinone anion. [s] 1,2-Bis(trimethylsilyl)benzene anion. [t] 1,4-Bis(trimethylsilyl)benzene anion. [u] N,N′-Bis(trimethylsilyl)-*p*-benzoquinonimine anion. [v] Tri-*tert*-butyl silyl. [w] Tris(trimethylsilyl)silyl. [x] 1,4-Bis(trimethylsilyl)naphthalene anion. [y] 1,5-Bis(trimethylsilyl)naphthalene anion. [z] 2,6-Bis(trimethylsilyl)naphthalene anion. [aa] 3,3,6,6-Tetrakis(trimethylsilyl)cyclohexa-1,4-diene cation. [bb] Tetrakis(trimethylsilylmethyl)ethene cation. [cc] UMP2/DZP//UHF/DZP. Ref 14, where DZP is a Dunning/Huzinaga full double-ζ basis set (DZ)[50] augmented with polarization functions (P).[53] [dd] UMP2/DZP//UHF/TZP. Ref 15, where TZP is a 6-311G** triple-ζ basis set (TZ)[51,52] supplemented with polarization functions (P).[53] [ee] UMP2/DZP//UHF/TZP. Ref 54. [ff] Prior theoretical study of this radical at higher level than calculated here has not appeared to our present knowledge.

($^1H_\alpha$) values are much smaller than those for the corresponding alkyl radicals, and the $a_{iso}(^1H_\beta)$ values are very small because of weak hyperconjugation.

The sign of $a_{iso}(^{29}Si_\alpha)$ is always negative in all the spin-bearing silicon atoms because of the minus sign of its magnetic moment and its positive spin density values. However, in the case of silicon in the β-position, $a_{iso}(^{29}Si_\beta)$ is positive and smaller. Moreover, when the electron is delocalized in the whole molecular system, the value of $a_{iso}(^{29}Si)$ is always small and positive in the anions (**10a**−**18a**, **21a**−**23a**) and larger and negative in the cations (**24a**−**25a**). Notice that the calculated signs for the hfcc's of ^{29}Si using the *Gaussian 03* program must be changed.[3] Shown in column C of Table 1, post-HF calculations were carried out by Guerra[14,15,54] using the MP2 method, in which the obtained $a_{iso}{}^{29}Si$ are always overestimated.

Phosphorus Radicals. The studied radicals containing ^{31}P nuclei are spread in a wide variety of systems. There are four neutral phosphinyl derivatives (**1b**, **2b**, **3b, 20b)**, in which the phosphorus is the spin-bearing atom. The $a_{iso}(^{31}P)$ values of these radicals are much lower than those of the other phosphorus spin-bearing atoms analyzed here, as occurs in the phosphoranyls **5b**−**9b** that present values of hfcc's ranging from 519 to 1371 G. The electron-withdrawing effect of oxygen and sulfur atoms provokes a drastic diminution in $a_{iso}(^{31}P)$ in other phosphoranyl radicals (**10b**−**13b**), whereas the presence of the methyl group (**18b**) and methoxy and phenyl groups (**23b**) does not decrease the characteristic high ^{31}P hfcc of phosphoranyl radicals. The optimized geometries for all the analyzed phosphoranyl present the characteristic bipyramidal trigonal (TBP) structure, as has been confirmed largely by means of EPR spectroscopy.[16−32] The two phosphinyl derivatives (**15b**, **21b**) present a pyramidal structure with the unpaired electron practically localized in the phosphorus nucleus, and thus, the hfcc's are high. The three studied cations (**4b**, **17b**, **22b**), derivatives of phosphine and diphosphine, also present high hfcc values for the same reason. In the aromatic radical anions (**16b**, **19b**, **24b**, **25b**), the unpaired electron is completely delocalized, and so, $a_{iso}(^{31}P)$ is relatively small. Finally, for radical **14b**, high hfcc values for ^{31}P and ^{19}F nuclei are obtained, as their hfcc's are very similar to radical **8b**, which presents an equivalent structure.

Sulfur Radicals. Analogously to the above nuclei, we have considered a variety of systems containing sulfur atoms. In five of them (**1c**, **2c**, **9c**, **24c**, **25c**), the sulfur is the spin-bearing atom. However, in contrast with the silicon and phosphorus nuclei, the $a_{iso}(^{33}S)$ values are much smaller, except for radicals **2c** and **9c**, in which the values are noticeable because of the high localization of the unpaired electron in the sulfur atom. In general, the relatively small value of the g_N factor of the ^{33}S nucleus gives rise to lower hfcc's than other nuclei in the same radical with similar spin densities. Radical **2c** is particularly interesting. Two possible configurations, trans and cis, have been considered here. The trans isomer has a pseudo-octahedral structure of C_{4v} symmetry in which the equatorial positions are occupied by four equivalent fluorines, one axial position is occupied by a doubly bonded oxygen, and the second axial position is occupied by the unpaired electron, whereas the cis isomer (C_s symmetry) has one equatorial oxygen ligand adjacent to the orbital containing the unpaired electron. We find at the B3LYP/TZVP//B3LYP/6-31G* level that the trans isomer is the most stable conformation by 10.8 kcal mol^{-1}. This result agrees with the results of Christe et al.,[73] and hence, it is the configuration considered in the hfcc calculations. Radical **24c** shows the typical T-shape of π-type sulfuranyl radicals in its most energetic stable conformation, and **25c** presents a planar arrangement between the sulfur atom and the phenyl ring. The other radicals studied here (**3c**, **4c**, **5c**, **7c**, **8c**, **10c**−**12c**, **14c**−**23c**) are conjugated cation radicals that show a very great delocalization of the unpaired electrons, and thus, the hfcc values are logically very small. The two conjugated anions considered (**6c**, **13c**) show the same behavior. Also, it is worth emphasizing that for this nucleus the natural abundance of the isotope with $I \neq 0$ (^{33}S) is very low (0.7%), which diminishes the precision of the experimental measurements for samples that are not isotopically enriched.

To our knowledge, only post-HF hfcc results of the sulfur nucleus have been found.[33] Thus, the present work is the first high-level calculations carried out on medium- and large-sized radicals containing sulfur.

Regression Analysis. The regression analysis has been divided into several subsets: (a) In the first one, we consider all the nuclei for which there are available experimental data and all their corresponding theoretical values (206 hfcc's); (b) in the next three, we consider all nuclei included in Tables 1, 2, and 3, respectively; (c) then, three additional subsets, each containing only one of the ^{29}Si, ^{31}P, and ^{33}S nuclei, have been considered; (d) the last subset includes only the above three nuclei of the third row.

In Figures 4 and 5, we depict the linear regression representing the calculated a_{iso}(G) values with the B3LYP functional with both TZVP and cc-pVQ(T)Z basis sets versus experimental a_{iso}-

TABLE 2: Theoretical Hyperfine Coupling Constants (G) of Radicals Containing ^{31}P Nuclei at (A) B3LYP/TZVP//B3LYP/6-31G* and (B) B3LYP/cc-pVQZ[a] (or cc-pVTZ[b])//B3LYP/6-31G* Levels.[c] (C) Other Theoretical Results

					a_{iso}(theoretical)			experimental	
no.	radical	state	energy (au)	nuclei	A	B	C	a_{iso}	ref
1b	$PH_2^{\bullet}$ [d]	$^{2}B_1$	−342.531631	^{31}P	76.9	60.2[a]	97.4[cc]	77.4	(55)
			(−342.545596)	$2\,^{1}H$	−13.3	−13.0	−17.2	17.5	
2b	$PF_2^{\bullet}$ [e]	$^{2}B_1$	−541.156396	^{31}P	96.9	72.1[a]	89.0[dd]	84.8	(56)
			(−541.200316)	$2\,^{19}F$	29.8	19.6	11.6	32.6	
3b	$PCl_2^{\bullet}$ [f]	$^{2}B_1$	−1261.832287	^{31}P	61.8	56.4[a]	71.8[ee]	68.3	(57)
			(−1261.88968)	$2\,^{35}Cl$	3.3	2.6	0.7	0.4	
4b	$PCl_3^{\bullet+}$ [g]	$^{2}A_1$	−1721.737146	^{31}P	720.6	761.1[a, hh]	763.3[ff]	833.5	(16)
			(−1721.821520)	$3\,^{35}Cl$	7.6	5.0	6.8	23.3	
5b	$PH_4^{\bullet}$ [h]	$^{2}A_1$	−343.686572	^{31}P	479.5	487.8[a]	499.9[ff]	519.3	(58)
			(−343.705318)	$2\,^{1}H_{ax}$	192.6	195.7	179.1	198.7	
				$2\,^{1}H_{eq}$	−6.5	−6.8	−8.6	6.0	
6b	$PH_3F^{\bullet}$ [i]	$^{2}A'$	−443.007974	^{31}P	702.6	701.9[a]	740.4[ff]	721.3	(58)
			(−443.039197)	^{19}F	330.6	289.3	317.4	347.2	
				$^{1}H_{ax}$	129.2	130.4	110.8	130.1	
				$2\,^{1}H_{eq}$	−11.6	−11.3	−15.0	12.6	
7b	$PHF_3^{\bullet}$ [j]	$^{2}A'$	−641.643917	^{31}P	931.5	954.6[a]	1044.3[ff]	1030.8	(58)
			(−641.703043)	$2\,^{19}F_{ax}$	195.5	182.4	206.1	226.8	
				$^{19}F_{eq}$	27.1	24.7	32.1	35.0	
				^{1}H	32.8	36.5	25.1	38.5	
8b	$PF_4^{\bullet}$ [k]	$^{2}A_1$	−740.960226	^{31}P	1203.3	1241.8[a]	1341.7[ff]	1330.0	(58)
			(−741.035614)	$2\,^{19}F_{ax}$	240.7	227.4	252.6	291.0	
				$2\,^{19}F_{eq}$	51.8	50.7	48.8	60.0	
9b	$PCl_3O^{\bullet-}$ [l]	$^{2}A'$	−1797.456933	^{31}P	1248.5	1314.2[a]	1537.8[ff]	1371.0	(59)
			(−1797.538824)	$2\,^{35}Cl_{ax}$	26.3	26.7	31.9	40.0	
				$^{35}Cl_{eq}$	26.4	26.8	38.3	20.0	
10b	$POS_3^{\bullet 2-}$ [m]	$^{2}A''$	−1611.319614	^{31}P	−12.5	−8.7[a]	−17.0[ff]	13.5	(60)
			(−1611.407255)						
11b	$PO_3F^{\bullet-}$ [n]	$^{2}A''$	−667.148785	^{31}P	−47.8	−41.9[a]	−38.2[ff]	39.1	(61)
			(−667.219863)	^{19}F	−12.4	−10.7	−9.1	8.0	
12b	$PO_2S_2^{\bullet 2-}$ [o]	$^{2}B_1$	−1288.344033	^{31}P	−12.7	−9.2[a]	−18.1[ff]	16.8	(60)
			(−1288.430210)						
13b	$PS_4^{\bullet 2-}$ [p]	$^{2}B_2$	−1934.291794	^{31}P	−12.5	−8.3[a]	−21.7[ff]	14.7	(60)
			(−1934.380103)						
14b	$PF_5^{\bullet-}$ [q]	$^{2}A_1$	−840.969709	^{31}P	1262.3	1290.5[a]	1364.7[ff]	1328.2	(62)
			(−841.044648)	$4\,^{19}F_{eq}$	182.2	172.7	175.5	206.6	
15b	$C_2H_6OP^{\bullet}$ [r]	$^{2}A'$	−496.470951	^{31}P	302.2	319.5[a]	413.7[ff]	375.0	(63)
			(−496.512910)	$6\,^{1}H$	4.2	4.5	4.7	5.6	
16b	$C_5H_5P^{\bullet-}$ [s]	$^{2}B_1$	−534.957419	^{31}P	32.6	31.1[a]	*gg*	35.6	(64)
			(−534.991978)	$^{1}H_{2,6}$	−4.1	−4.1		3.7	
				$^{1}H_4$	−8.2	−8.0		7.6	
				$^{13}C_4$	9.3	7.2		12.0	
17b	$C_3H_9P^{\bullet+}$ [t]	$^{2}A_1$	−460.880802	^{31}P	322.1	322.2[a]	394.7[ff]	388.9	(17)
			(−460.913545)	$9\,^{1}H$	12.4	12.4	10.6	12.1	
18b	$C_3H_{10}P^{\bullet}$ [u]	$^{2}A'$	−461.688947	^{31}P	469.1	475.2[a]	*gg*	484.0	(65)
			(−461.721224)	^{1}H	170.2	172.1		182.0	
19b	$C_9H_7P^{\bullet-}$ [v]	$^{2}A''$	−688.661860	^{31}P	22.4	19.8[a]	*gg*	23.6	(66)
			(−688.714729)						
20b	$C_{12}H_{10}P^{\bullet}$ [w]	$^{2}B_1$	−804.780800	^{31}P	61.9	70.0[b]	*gg*	78.7	(67)
			(−804.808590)						
21b	$C_{12}H_{10}OP^{\bullet}$ [x]	^{2}A	−880.055379	^{31}P	297.3	312.9[b]	*gg*	361.6	(68)
			(−880.085145)						
22b	$C_6H_{18}P_2^{\bullet+}$ [y]	$^{2}A_u$	−922.092176	$2\,^{31}P$	439.5	459.2[b]	*gg*	482.0	(69)
			(−922.125141)	$2\,^{1}H_{\beta}$	19.5	19.3		∼20[ii]	
23b	$C_{10}H_{16}P^{\bullet}$ [z]	^{2}A	−807.400458	^{31}P	508.7	530.4[b]	*gg*	557.0	(70)
			(−807.424505)	$^{1}H_{ax}$	119.5	118.8		126.5	
				$^{1}H_{eq}$	−10.6	−10.5		10.2	
24b	$C_{23}H_{17}P^{\bullet-}$ [aa]	$^{2}B_1$	−1228.359099	^{31}P	31.0	38.9[b]	*gg*	33.1	(71)[jj]
25b	$C_{17}H_{29}P^{\bullet-}$ [bb]	$^{2}A''$	−1006.870705	^{31}P	20.0	29.6[b]	*gg*	29.4	(64)
			(−1006.894012)						

[a] (B3LYP/cc-pVQZ//B3LYP/6-31G*). [b] (B3LYP/cc-pVTZ//B3LYP/6-31G*). [c] The corresponding energies are shown in parentheses. [d] Phosphinyl. [e] Difluorophosphinyl. [f] Dichlorophosphinyl. [g] Trichlorophosphine cation. [h] Phosphoranyl. [i] Fluorophosphoranyl. [j] Trifluorophosphoranyl. [k] Tetrafluorophosphoranyl. [l] Trichlorooxophosphoranyl anion. [m] Trisulfuroxophosphoranyl dianion. [n] Trioxofluorophosphoranyl anion. [o] Dioxodisulfurphosphoranyl dianion. [p] Tetrasulfurphosphoranyl dianion. [q] Phosphorus pentafluoride anion. [r] Dimethylphosphonyl. [s] Phosphabenzene anion. [t] Trimethylphosphine cation. [u] Trimethylphosphoranyl. [v] 2-Phosphanaphthalene anion. [w] Diphenylphosphinyl. [x] Diphenylphosphonyl. [y] 1,1′-Bis-trimethyldiphosphine cation. [z] Ter-*tert*-butoxidihidro(phenyl)phosphoranyl. [aa] 2,4,6-Triphenylphosphabenzene anion. [bb] 2,4,6-Tri-*tert*-butylphosphabenzene anion. [cc] UQCISD/usp6-311+G(2df,p) on P//UQCISD/6-311G(d,p). Ref 4. [dd] UQCISD/6-311+G(2df,p)//UQCISD/6-311G(d,p). Ref 4. [ee] UQCISD/6-311+G(2d,p)//UQCISD/6-311G(d,p). Ref 4. [ff] MP2/6-311G**//MP2/6-31G**. Ref 7. [gg] Prior theoretical study of this radical at higher level than calculated here has not been found up to the present. [hh] We carried out calculations at highest level to confirm the anomalous values of the chlorine nuclei as suggested by Cramer et al. (ref 7). The obtained $a_{iso}(^{31}P)$ and $a_{iso}(^{35}Cl)$ are as follows. (a) UQCISD/6-311G(d,p)//UMP2/6-311G(d,p): 767.5 G, 6.7 G. (b) MP4(SDTQ)/6-311++G(d,p)//MP2/6-311G(d,p): 803.7 G, 4.2 G. (c) MP2/6-311G(d,p)//MP2/6-311G(d,p): 802.9 and 4.1 G, respectively. [ii] The experimental measurements demonstrate that only 2 of the 18 H(β) show hyperfine splitting.[69] In the present calculations, two possible conformations (eclipsed and staggered) have been taken into account. The staggered structure is the energetically most favorable and gives rise to only two hfcc values for the protons in close agreement with the experimental ones. [jj] For this radical, the only value of hfcc measured with precision is the value corresponding to the ^{31}P nucleus. The hfcc's of protons are only estimated, so that they have not been included in this table.

TABLE 3: Theoretical Hyperfine Coupling Constants (G) of Radicals Containing ^{33}S Nuclei at (A) B3LYP/TZVP//B3LYP/6-31G* and (B) B3LYP/cc-pVQZ[a] (or cc-pVTZ[b])//B3LYP/6-31G* Level.[c] (C) Other Theoretical Results.

					a_{iso} (theoretical)			experimental	
no.	radical	state	energy (au)	nuclei	A	B	C	a_{iso}	ref
1c	$CH_3OS^{\bullet}$ [d]	$^2A''$	−513.344193	^{33}S	7.8	7.5[a]	*cc*	8.0	(72)
			(−513.384300)	$3\,^{1}H$	8.6	10.0		11.6	
2c	$SF_4O^{\bullet -}$ [e]	$^2A_1$	−872.985857	^{33}S	314.3	335.7[a]	*cc*	362.6	(73)
			(−873.066263)	$4\,^{19}F$	136.4	135.2		189.5	
3c	$C_2H_2NS_2^{\bullet}$ [f]	$^2B_1$	−928.558961	$2\,^{33}S$	3.4	3.2[a]	3.3[dd]	4.2	(74)
			(−928.617706)	^{14}N	8.3	6.6	11.20	10.7	
				$2\,^{1}H$	−1.2	−1.1	−0.7	1.4	
4c	$C_2N_3S_3^{\bullet}$ [g]	$^2B_1$	−1435.083854	$2\,^{33}S$	2.2	2.1[a]	*cc*	3.3	(75)
			(−1435.179284)	^{14}N	8.5	6.8		11.2	
				$2\,^{14}N$	0.6	0.5		0.8	
5c	$C_4N_3S_2^{\bullet}$ [h]	$^2B_1$	−1113.084187	$2\,^{33}S$	3.4	3.1[a]	*cc*	4.4	(76)
			(−1113.158541)	^{14}N	8.9	7.0		12.1	
6c	$NO_7S_2^{\bullet 2-}$ [i]	$^2B_1$	−1377.817338	$2\,^{33}S$	−2.1	−2.0[a]	*cc*	1.3	(77)
			(−1377.988067)	^{14}N	10.6	9.0		13.0	
7c	$C_4H_4S_2^{\bullet +}$ [j]	$^2B_{3u}$	−950.991842	$2\,^{33}S$	7.9	7.1[a]	*cc*	9.8	(78)
			(−951.005104)	$4\,^{1}H$	−3.0	−2.9		2.8	
8c	$C_6H_4NS_2^{\bullet}$ [k]	$^2B_1$	−1082.258088	$2\,^{33}S$	3.1	2.7[a]	*cc*	3.9	(74)
			(−1082.329918)	^{14}N	8.7	6.9		11.0	
				$4\,^{1}H_{av}$	−0.6	−0.5		0.6	
9c	$C_6H_5O_2S^{\bullet}$ [l]	$^2A'$	−780.351306	^{33}S	61.2	65.8[a]	*cc*	83.2	(79)
			(−780.433711)	$2\,^{1}H_o$	1.0	1.0		1.1	(80)
				$2\,^{1}H_m$	0.5	0.5		0.3	
				$^{1}H_p$	−0.4	−0.4		0.5	
10c	$C_6H_4S_4^{\bullet +}$ [m]	$^2B_{3u}$	−1823.667990	$4\,^{33}S$	3.5	3.2[a]	*cc*	4.3	(81)
			(−1823.769840)	$4\,^{1}H$	−1.3	−1.2		1.3	
				$^{13}C_{1,2}$	1.6	1.0		2.9	
11c	$C_6H_4S_4^{\bullet +}$ [n]	$^2A_1$	−1823.624053	$4\,^{33}S$	3.5	3.1[a]	*cc*	4.2	(82)
			(−1823.724972)	^{41}H	−1.2	−1.1		0.3	
12c	$C_8H_6S_2^{\bullet +}$ [o]	$^2B_1$	−1104.699285	$2\,^{33}S$	7.6	6.4[a]	*cc*	9.4	(78)
			(−1104.768724)	$^{1}H_{2,3}$	−3.1	−2.9		3.3	
				$^{1}H_{5,8}$	<0.1	−0.3		0.2	
				$^{1}H_{6,7}$	−1.2	−1.3		1.1	
13c	$C_8O_4S_4^{\bullet -}$ [p]	$^2A_2$	−2198.881401	$^{33}S_{2,6}$	−0.8	−0.8[b]	*cc*	0.8	(83)
			(−2198.942731)	$^{33}S_{4,8}$	−1.0	−1.1		1.4	
				$^{13}C_{1,3,5,7}$	−2.3	−2.5		2.0	
				$^{13}C_{3a,4a,7a,8a}$	2.9	1.0		4.1	
				$4\,^{17}O$	−2.2	−1.4		3.6	
14c	$C_{10}H_6S_2^{\bullet +}$ [q]	$^2A_2$	−1180.975563	$2\,^{33}S$	5.2	5.9[b]	*cc*	7.2	(84)
			(−1181.014295)	$^{1}H_{3,8}$	−4.0	−3.8		4.6	
				$^{1}H_{4,7}$	1.0	1.0		1.0	
				$^{1}H_{5,6}$	−5.4	−5.0		5.5	
15c	$C_{10}H_4S_4^{\bullet +}$ t[r]	^2A_u	−1976.196989	$^{33}S_{1,2,5,6}$	3.6	4.2[b]	*cc*	4.4	(84)
			(−1976.270890)	$^{1}H_{3,4,7,8}$	−1.3	−1.2		1.5	
16c	$C_{12}H_8OS^{\bullet +}$ [s]	$^2B_1$	−935.426922	^{33}S	8.4	9.3[b]	*cc*	11.9	(78)
			(−935.462232)	$^{1}H_{1,8}$	−0.1	−0.1		0.6	
				$^{1}H_{2,7}$	−1.3	−1.2		1.0	
				$^{1}H_{3,6}$	−1.8	−1.8		2.1	
				$^{1}H_{4,5}$	0.3	0.3		0.3	
17c	$C_{12}H_8S_2^{\bullet +}$ [t]	$^2A_1$	−1258.394958	$2\,^{33}S$	7.1	7.8[b]	*cc*	9.2	(78)
			(−1258.441314)	$^{1}H_{1,4,5,8}$	0.1	<0.1		0.1	
				$^{1}H_{2,3,6,7}$	−1.3	−1.2		1.3	
18c	$C_{14}H_8S_2^{\bullet +}$ [u]	^2A_u	−1334.657921	$2\,^{33}S$	4.4	5.0[b]	*cc*	5.3	(85)
			(−1334.706181)	$^{1}H_{2,7}$	−2.1	−1.9		1.8	
				$^{1}H_{3,8}$	−1.1	−1.1		1.3	
				$^{1}H_{5,10}$	−1.5	−1.4		1.7	
				$^{1}H_{4,9}$	−1.1	−1.0		1.3	
19c	$C_{14}H_8S_2^{\bullet +}$ [v]	$^2B_1$	−1334.626477	$^{33}S_{1,4}$	6.2	6.9[b]	*cc*	8.3	(86)
			(−1334.669514)	$^{1}H_{2,3}$	−1.9	−1.7		2.1	
				$^{1}H_{5,10}$	−0.3	−0.3		0.3	
				$^{1}H_{7,8}$	−0.7	−0.7		0.5	
20c	$C_{14}H_8S_4^{\bullet +}$ [w]	$^2A_1$	−2131.073034	$4\,^{33}S$	3.3	3.7[b]	*cc*	4.1	(81)[ee]
			(−2131.145515)	$^{1}H_{10,11,14,15}$	−0.5	−0.5		0.5	
				$^{1}H_{9,12,13,16}$	−0.1	−0.1		0.2	
21c	$C_{10}H_{12}S_4^{\bullet +}$ [x]	$^2B_{1u}$	−1981.005607	$4\,^{33}S$	3.2	3.6[b]	*cc*	4.0	(81)
			(−1981.076234)	$12\,^{1}H$	0.9	0.8		0.7	
22c	$C_{18}H_{10}S_2^{\bullet +}$ [y]	$^2B_1$	−1488.347465	$2\,^{33}S$	4.1	4.5[b]	*cc*	4.6	(85)[ee]
			(−1488.393739)	$^{1}H_{1,12}$	−0.8	−0.7		0.9	
				$^{1}H_{2,11}$	−2.6	−2.5		2.5	
				$^{1}H_{5,8}$	−0.7	−0.6		0.7	
				$^{1}H_{4,9}$	−0.2	−0.2		0.3	
				$^{1}H_{6,7}$	−0.8	−0.8		0.9	

TABLE 3: (Continued)

					a_{iso}(theoretical)			experimental	
no.	radical	state	energy (au)	nuclei	A	B	C	a_{iso}	ref
23c	$C_{18}H_8S_4^{\bullet+}$ [z]	$^2A_2$	−2283.579796	$4^{33}S$	2.4	2.9[b]	*cc*	3.4	(84)
			(−2283.664682)	$^1H_{4,5,10,11}$	−0.5	−0.4		0.6	
				$^1H_{3,6,9,12}$	−0.7	−0.7		0.6	
24c	$C_{10}H_3O_2F_{12}S^{\bullet}$ [aa]	$^2A''$	−2363.789244	^{33}S	11.0	12.7[b]	*cc*	15.7	(87)[ff]
			(−2363.799853)	2^1H_m	0.7	0.6		0.8	
				9^1H	0.1	0.1		0.2	
				$12^{19}F$	0.7	0.6		0.6	
25c	$C_{18}H_{29}S^{\bullet}$ [bb]	$^2A'$	−1101.074941	^{33}S	16.8	15.2[b]	*cc*	14.8	(88)
			(−1101.821176)						

[a] (B3LYP/cc-pVQZ//B3LYP/6-31G*). [b] (B3LYP/cc-pVTZ//B3LYP/6-31G*). [c] The corresponding energies are shown in parentheses. [d] Methylsulfinyl. [e] Tetrafluoro-λ⁴-sulfane oxide anion. [f] 1,3,2-Dithiazo-2-yl. [g] 1,3,5-Trithia-2,4,6-triazapentalenyl. [h] 4,5-Dicyano-1,3,2-dithiazo-2-yl. [i] Peroxylamine disulfonate dianion. [j] 1,4-Dithiin cation. [k] 1,3,2-Benzodithiazolyl. [l] Phenylsulfonyl. [m] Tetrathia-tetrahydrofulvalene cation. [n] 1,4,5,8-Tetrathiatetraline cation. [o] Benzo-1,4-dithiin cation. [p] Dithieno[3,4-b;3′,4′-e]paradithiin-1,3,5,7-tetraone anion. [q] 1,2-Dithiaacenaphtene cation. [r] 1,2,5,6-Tetrathiapyracene cation. [s] Phenoxathiine cation. [t] Thianthrene cation. [u] 1,6-Dithio-1,6-dihydropyrene cation. [v] Acenaphtho[1,2-b][1,4]dithine cation. [w] Dibenzo−TTF cation. [x] Tetramethyl−TTF cation. [y] 3,10-Dithia-3,10-dihydroperylene cation. [z] 1,2,5,6-Tetrathiadibenzo[c,i]pyracene cation. [aa] 4-*tert*-Butyl-2,2,6,6-tetrakis(trifluoromethyl)-6,8-dihydro-2*H*-λ³-[1,2]oxathiolo[4,3,2-*hi*][2,1]benzoxathiole. [bb] 2,4,6-Tri-*tert*-butylphenylthiyl. [cc] Prior theoretical study of this radical at higher level than calculated here has not been found up to the present. [dd] B3LYP/6-31G(df,p)//B3LYP/6-31G(d). Ref 33. [ee] New assignment. [ff] In the original paper, one ^{13}C hfcc of 9.9 G is given for C_1, obtained for spectrum simulation approach, supposing the natural abundance (1.1%) of ^{13}C. The calculations, however, give rise to higher spin densities at the four carbons supporting the fluorine atoms other than the C_1. We think that the procedure to obtain the hfcc of ^{13}C is not well-supported. For this reason, it is not included in this table.

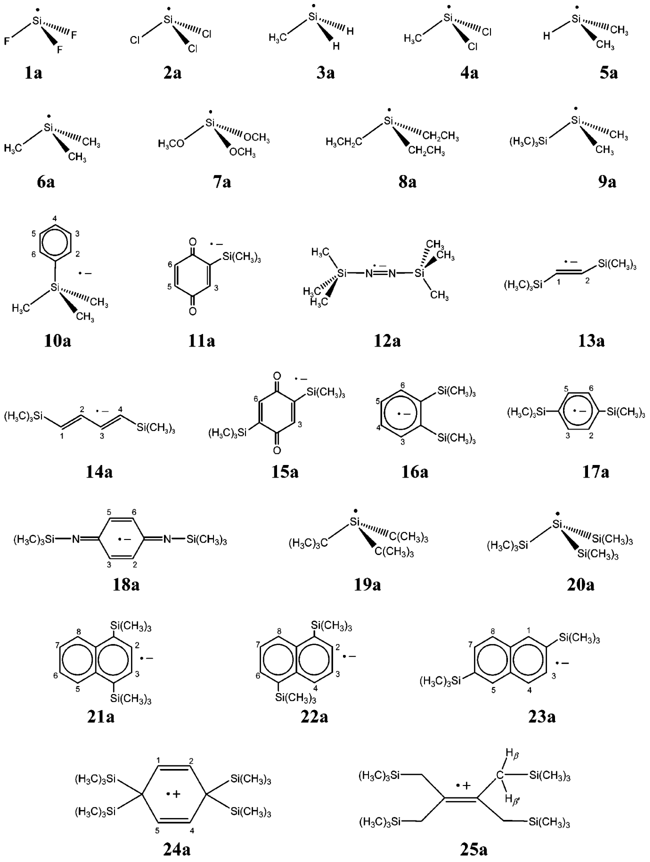
1a **2a** **3a** **4a** **5a** **6a** **7a** **8a** **9a** **10a** **11a** **12a** **13a** **14a** **15a** **16a** **17a** **18a** **19a** **20a** **21a** **22a** **23a** **24a** **25a**

Figure 1. Geometrical structures of radicals containing ^{29}Si nuclei.

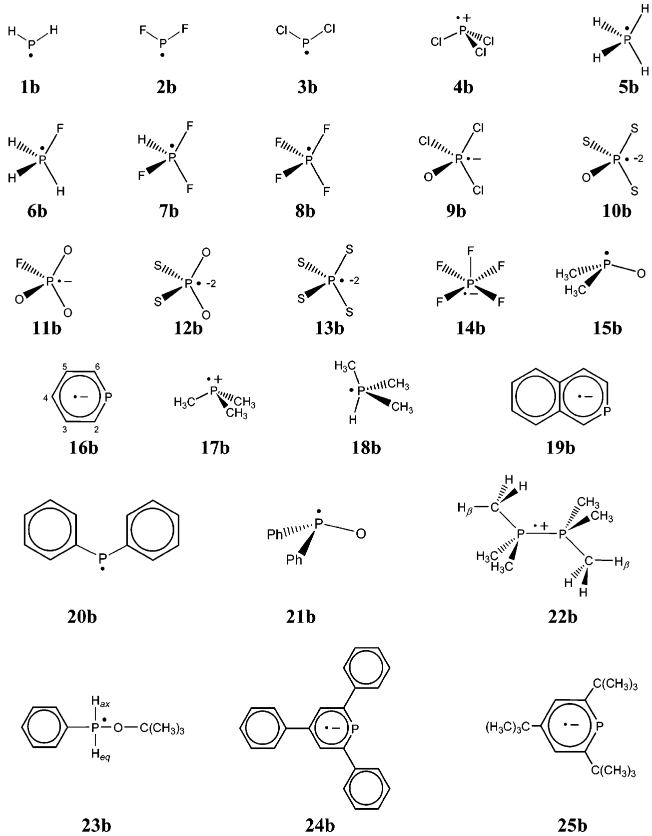
1b **2b** **3b** **4b** **5b** **6b** **7b** **8b** **9b** **10b** **11b** **12b** **13b** **14b** **15b** **16b** **17b** **18b** **19b** **20b** **21b** **22b** **23b** **24b** **25b**

Figure 2. Geometrical structures of radicals containing ^{31}P nuclei.

(G) values for the first subset (all nuclei) and the last subset (^{29}Si, ^{31}P, and ^{33}S nuclei), respectively. In each figure, we represent the points of the corresponding hfcc values, the bisectrix (solid line), and both slopes of linear regression (dotted line for TZVP and dashed line for cc-pVQ(T)Z). Moreover, to clarify the above representation, we enclose an amplified area ranging from 0 to 25 G.

Results of linear regression analysis for the subsets described above and considering both TZVP and cc-pVQ(T)Z basis sets are summarized in Table 4. This table contains seven well-defined columns, corresponding to the regression analysis of the eight subsets considered. The first column shows the name of the subset, the second gives the number of points (N) considered for the regression analysis, and the rest of the columns correspond to the results of this analysis: slope, intercept, correlation coefficient (R^2), mean absolute deviation (MAD), and range data. The MAD only considers the absolute value, so that all deviations are converted to positive numbers, added, and then averaged. We have defined the employed MAD for our calculations in the bottom of Table 4. It is important to notice that error expressed as a percentage basis is very coherent and intuitive, but this procedure gives rise to serious difficulties with hfcc's that are very small or nearly zero. For this reason,

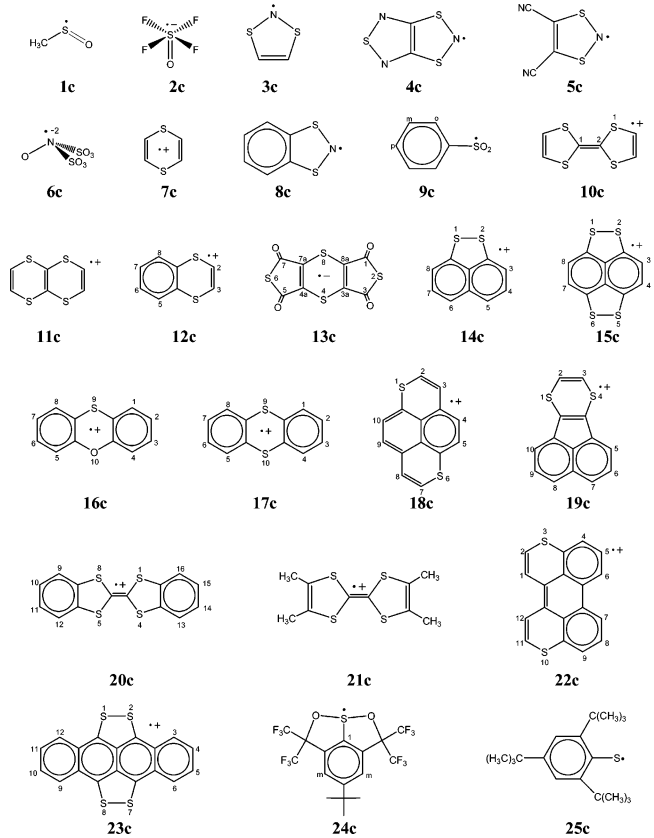

Figure 3. Geometrical structures of radicals containing ^{33}S nuclei.

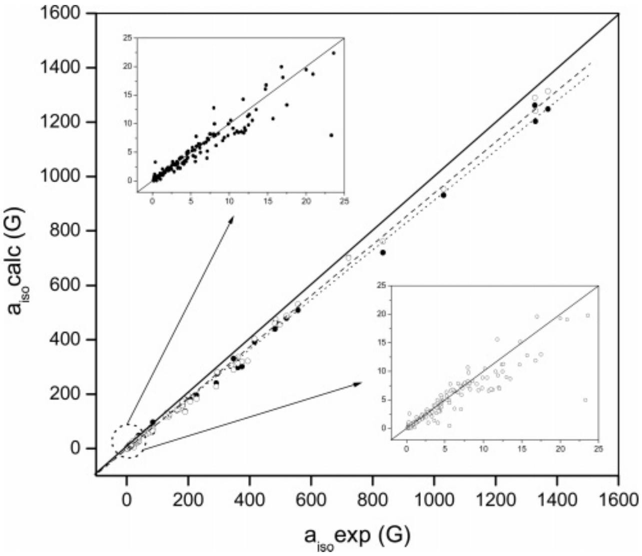

Figure 4. Plot of theoretical vs experimental hfcc's for all nuclei of studied radicals, calculated using B3LYP/TZVP//B3LYP/6-31G* (full circles) and B3LYP/cc-pVQ(T)Z//B3LYP/6-31G* (open circles). In this figure, the linear fits are indicated by dotted line for the TZVP basis set and by dashed line for the cc-pVQ(T)Z one. The parameters of the best linear functions are listed in Table 4. The insets expand the region from 0 to 25 G.

we think that this methodology for manipulating errors is not adequate in this study, because we have a very wide range of hfcc's and some of them have extremely small values.

In general, both DFT schemes yield hfcc's reasonably close to the experimental values. All the R^2 values are higher than 0.9988, except for nuclei of sulfur compounds, in which R^2 ranges between 0.9947 and 0.9969.

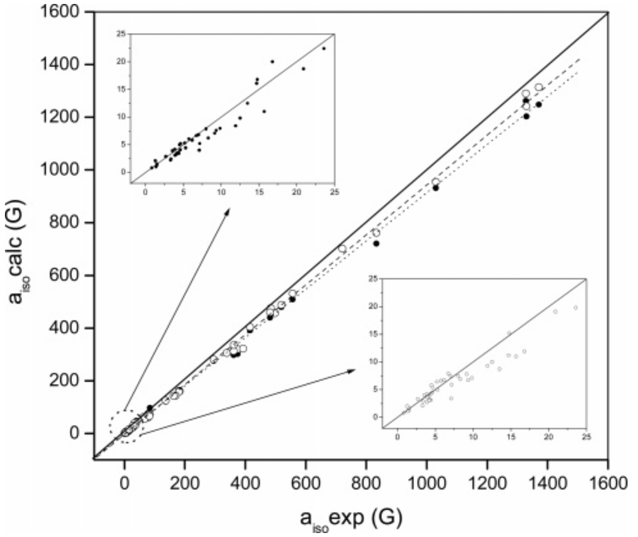

Figure 5. Plot of theoretical vs experimental hfcc's for ^{29}Si, ^{31}S, and ^{33}S nuclei of studied radicals, calculated using B3LYP/TZVP//B3LYP/6-31G* (full circles) and B3LYP/cc-pVQ(T)Z//B3LYP/6-31G* (open circles). In this figure, the linear fits are indicated by dotted line for the TZVP basis set and by dashed line for the cc-pVQ(T)Z one. The parameters of the best linear functions are listed in Table 4. The insets expand the region from 0 to 25 G.

TABLE 4: Regression Analysis for Predictions of hfcc's (G) at (A) B3LYP/TZVP//B3LYP/6-31G* and (B) B3LYP/cc-pVQ(T)Z/B3LYP/6-31G* Levels

	N	slope	intercept	R^2	MAD[a]	range
(A) B3LYP/TZVP//B3LYP/6-31G*						
all nuclei	206	0.913	−0.61	0.9990	8.2	1371
all nuclei of Table 1	75	0.913	0.09	0.9995	3.9	498
all nuclei of Table 2	52	0.916	−1.31	0.9988	23.4	1371
all nuclei of Table 3	79	0.832	−0.21	0.9969	2.3	363
only ^{29}Si nucleus	26	0.925	−0.79	0.9989	9.9	498
only ^{31}P nucleus	25	0.917	−2.32	0.9986	38.6	1358
only ^{33}S nucleus	26	0.862	−0.54	0.9993	3.9	363
(^{29}Si, ^{31}P, ^{33}S) nuclei	77	0.915	−1.42	0.9990	18.9	1371
(B) B3LYP/cc-pVQ(T)Z//B3LYP/6-31G*						
all nuclei	206	0.940	−1.90	0.9990	7.2	1371
all nuclei of Table 1	75	0.922	−0.04	0.9991	3.9	498
all nuclei of Table 2	52	0.948	−6.34	0.9989	19.8	1371
all nuclei of Table 3	79	0.878	−0.56	0.9947	2.1	363
only ^{29}Si nucleus	26	0.916	0.94	0.9994	9.2	498
only ^{31}P nucleus	25	0.952	−7.56	0.9991	27.9	1358
only ^{33}S nucleus	26	0.922	−0.82	0.9994	2.7	363
(^{29}Si, ^{31}P, ^{33}S) nuclei	77	0.946	−3.06	0.9993	14.2	1371

[a] MAD (mean absolute deviation), defined as $(1/N)\Sigma_i^N|a_{iso}(calc) - a_{iso}(exp)|$.

The slopes are close to 0.91 and 0.95 in both basis sets when all nuclei are considered. These slopes improve a great amount when Dunning's basis sets are used. However, for all nuclei of sulfur compounds, these large basis sets yield slopes lower than 0.9. The larger the rate range/MAD is, the lower the errors. The ranges of the compared hfcc's for phosphorus compounds is very wide (1371 G), whereas for sulfur compounds, it is smaller (363 G). The best values of hfcc's are obtained for sulfur compounds, because the rate range/MAD is larger (157.8 with TZVP and 172.9 with cc-pVQ(T)Z) than for silicon (127.7 for both basis sets) and phosphorus (58.6 and 69.2, respectively) compounds. The complete analysis for all nuclei can be considered excellent, because with 206 hfcc values, the rate range/MAD is the highest for both basis sets (167.2 and 190.4, respectively).

For three nuclei of the third row, ^{29}Si, ^{31}P, and ^{33}S, we have carried out a more complete analysis, obtaining good agreement between calculated and experimental data. The analysis for the third-row nuclei gives rise to similar results that when all nuclei are considered. The regression analysis yields slopes from 0.862 to 0.925 using the TZVP basis set and rises to 0.952 using the cc-pVQ(T)Z basis set. We think that the values compared in this work (77 hfcc's) comprise a large amount of data and it can be considered a significant statistic. The rate range/MAD is higher for sulfur nuclei with similar behavior to the subsets above considered for all nuclei of Tables 1−3 (^{29}Si, ^{31}P, and ^{33}S).

Several points should be singled out for comments about the chlorine nucleus from Figure 4. As can be seen in the insets of this figure, there is a point far away from the other points, which are closely spread around the ideal line, that corresponds to the ^{35}Cl nucleus in Cl_3P^+ (**4b**). This discrepancy may possibly be due to the interactions of this radical with the matrix used in the experimental measurements, as Cramer et al.[7] have also suggested previously. On the other hand, the interaction of the unpaired electron with the large nuclear quadrupole of the ^{35}Cl nucleus makes the accurate determination of hfcc's very difficult.[29a] To gain insight into the origin of this discrepancy, other calculations at higher computational levels have been carried out, leading to the data shown in the bottom of Table 2. As can be seen, all the calculations give rise to hfcc values for the ^{35}Cl nucleus in the range 4−7 G, very far from the data reported in ref 16. These theoretical results suggest that the corresponding experimental value should be revised.

Conclusions

A significant attempt to compare theoretical and experimental a_{iso} values of nuclei of the third row using DFT methods has been carried out. For this set of 75 radicals, 206 experimental hfcc's are available for 8 different nuclei of the first, second, and third rows, of which 77 data points correspond to a_{iso}(^{29}Si, ^{31}P, and ^{33}S). In the case of the ^{35}Cl nucleus, the number of hfcc's included is not sufficient to obtain conclusions. For this nucleus, there are very few data available in the literature.

DFT theory provides reliable predictions of the hfcc's of radicals even when not very large basis sets are used. The influence of the basis set appears to be more important than the hybrid functional used. On the other hand, the geometries of radicals are not very sensitive to the size of the basis set used in the geometry optimization. However, the conformational changes play an important role in the computation of hfcc's of some radicals, for which the optimized conformation used can be deduced by the symmetry data given in each table.

If we take into account the conclusions of ref 3, the EPR-III basis set,[34a,b] in conjunction with the B3LYP hybrid functional, is the most useful scheme for hfcc calculation for nuclei of the first two rows, but it is not applicable to nuclei of the third row, because it has not been parametrized for them yet. For this reason, we think that the combination of the B3LYP functional with a TZVP basis set results in an excellent predictor of hfcc's for radicals of moderate and large size, including nuclei of the first, second, and third rows. The latter basis set provides hfcc values which as closer to the experimental ones as those obtained with the cc-pVQ(T)Z basis sets.

Acknowledgment. This work has been supported by the grant BQU2002-00582 of the Dirección General de Política Científica of MCyT (Spain).

References and Notes

(1) (a) Carrington, A.; McLachlan, A. D., *Introduction to Magnetic Resonance*; Harper and Row: New York, 1967. (b) Orton, J. W. *Electron Paramagnetic Resonance*; Gordon and Breach Science Publishers: New York, 1968. (c) Abraham, A.; Bleany, B. *Electron Paramagnetic Resonance of Transitions Ions*; Clarendon Press: Oxford, England, 1970. (d) Gerson, F. *High-Resolution ESR Spectroscopy*; Wiley: New York, 1970. (e) Atherton, N. M. *Principles of Electron Spin Resonance*; Ellis Horwood: New York, 1993. (f) Harriman, J. E. *Theoretical Foundations of Electron Spin Resonance*; Academic Press: New York, 1978. (g) Slichter, C. P. *Principles of Magnetic Resonance*, 3rd ed.; Springer-Verlag: Berlin, 1990. (h) Mabbs, F. E.; Collison, D. *Electron Paramagnetic Resonance of d Transition Metal Compounds*; Elsevier: Amsterdam, 1992. (i) Weil, J. A.; Bolton; J. R., Wertz, J. E.; *Electron Spin Resonance. Elementary and Practical Applications*; Wiley-Interscience: New York. 1994. (j) Gerson, F.; Huber, W. *Electron Spin Resonance Spectroscopy of Organic Radicals*; Wiley-VCH: Weinheim, Germany, 2003.

(2) Kaupp, M., Bühl, M., Malkin, V. G., Eds. *Calculation of NMR and EPR Parameters. Theory and Applications*; Wiley-VCH: Weinheim, 2004.

(3) (a) Hermosilla, L.; Calle, P.; Garcia de la Vega, J. M.; Sieiro, C. *J. Phys. Chem. A* **2005**, *109*, 1114. (b) Hermosilla, L.; Calle, P.; Sieiro, C. *Phosphorus, Sulfur Silicon Relat. Elem.* **2005**, *180*, 1421.

(4) Nguyen, M. T.; Creve, S.; Eriksson, L. A.; Vanquickenborne, L. G. *Mol. Phys.* **1997**, *91*, 537.

(5) Nguyen, M. T.; Creve, S.; Vanquickenborne, L. G. *J. Phys. Chem.* **1997**, *101*, 3174.

(6) Cramer, C. J. *Essentials of Computational Chemistry. Theories and Models*; Wiley: Chichester, 2002.

(7) Cramer, C. J.; Lim, M. H. *J. Phys. Chem.* **1994**, *98*, 5024.

(8) Kaszynski, P. *J. Phys. Chem. A* **2001**, *105*, 7615.

(9) (a) Becke, A. D. *J. Chem. Phys.* **1993**, *98*, 5648. (b) Lee, C.; (b) Yan, W.; Parr, R. G. *Phys. Rev. B* **1998**, *37*, 785.

(10) Godbout, N.; Salahub, D. R.; Andzelm, J.; Wimmer, E. *Can. J. Chem.* **1992**, *70*, 560.

(11) Wood, D. E.; Dunning, T. H. *J. Chem. Phys.* **1993**, *98*, 1914. Peterson, K. A.; Kendall, R. A.; Dunning, T. H. *J. Chem. Phys.* **1993**, *99*, 1930. Peterson, K. A.; Kendall, R. A.; Dunning, T. H. *J. Chem. Phys.* **1993**, *99*, 9790.

(12) Frisch, M. J.; Trucks, G. W.; Schlegel, H. B.; Scuseria, G. E.; Robb, M. A.; Cheeseman, J. R.; Montgomery, Jr., J. A.; Vreven, T.; Kudin, K. N.; Burant, J. C.; Millam, J. M.; Iyengar, S. S.; Tomasi, J.; Barone, V.; Mennucci, B.; Cossi, M.; Scalmani, G.; Rega, N.; Petersson, G. A.; Nakatsuji, H.; Hada, M.; Ehara, M.; Toyota, K.; Fukuda, R.; Hasegawa, J.; Ishida, M.; Nakajima, T.; Honda, Y.; Kitao, O.; Nakai, H.; Klene, M.; Li, X.; Knox, J. E.; Hratchian, H. P.; Cross, J. B.; Bakken, V.; Adamo, C.; Jaramillo, J.; Gomperts, R.; Stratmann, R. E.; Yazyev, O.; Austin, A. J.; Cammi, R.; Pomelli, C.; Ochterski, J. W.; Ayala, P. Y.; Morokuma, K.; Voth, G. A.; Salvador, P.; Dannenberg, J. J.; Zakrzewski, V. G.; Dapprich, S.; Daniels, A. D.; Strain, M. C.; Farkas, O.; Malick, D. K.; Rabuck, A. D.; Raghavachari, K.; Foresman, J. B.; Ortiz, J. V.; Cui, Q.; Baboul, A. G.; Clifford, S.; Cioslowski, J.; Stefanov, B. B.; Liu, G.; Liashenko, A.; Piskorz, P.; Komaromi, I.; Martin, R. L.; Fox, D. J.; Keith, T.; Al-Laham, M. A.; Peng, C. Y.; Nanayakkara, A.; Challacombe, M.; Gill, P. M. W.; Johnson, B.; Chen, W.; Wong, M. W.; Gonzalez, C.; Pople, J. A. *Gaussian 03*, Revision B.03; Gaussian, Inc., Pittsburgh, PA, 2004.

(13) Apeloig, Y.; Bravo-Zhivotovskii, D.; Yuzefovich, M.; Bendikov, M.; Shames, A. I. *Appl. Magn.* Reson. **2000**, *18*, 425.

(14) Guerra, M. *J. Am. Chem. Soc.* **1993**, *115*, 11926.

(15) Guerra, M. *Chem. Phys. Lett.* **1995**, *246*, 251.

(16) Aagaard, O. M.; Waal, B. F. M. D.; Cabbolet, M. J. T. F.; Janssen, R. A. T. *J. Phys. Chem.* **1992**, *96*, 614.

(17) Janssen, R. A. J.; Aagaard, O. M.; van der Woerd, M. J.; Buck, H. M. *Chem. Phys. Lett.* **1990**, *171*, 127.

(18) Bentrude, W. G. *Acc. Chem. Res.* **1982**, *15*, 117.

(19) Davies, A. G.; Griller, D.; Roberts, B. P. *J. Chem. Soc., Perkin Trans. 2* **1972**, 993.

(20) Giles, J. R. M.; Roberts, B. P. *J. Chem. Soc., Perkin Trans. 2* **1981**, 1211.

(21) (a) Nakanishi, A.; Nishikida, K.; Bentrude, W. G. *J. Am. Chem. Soc.* **1978**, *100*, 6403. (b) Nakanishi, A.; Nishikida, K.; Bentrude, W. G. *J. Am. Chem. Soc.* **1978**, *100*, 6398.

(22) Watts, G. B.; Griller, D.; Ingold, K. U. *J. Am. Chem. Soc.* **1972**, *94*, 8784.

(23) Aagaard, O. M.; Janssen, R. A. J.; Buck, H. M. *Recl. Trav. Chim. Pays-Bas* **1989**, *108*, 262.

(24) Aagaard, O. M.; Janssen, R. A. J.; Waal, B. F. M. D.; Buck, H. M. *J. Am. Chem. Soc.* **1990**, *112*, 938.

(25) Berclaz, T.; Geoffroy, M.; Lucken, E. A. C. *Chem. Phys. Lett.* **1975**, *36*, 677.

(26) Colussi, A. J.; Morton, J. R.; Preston, K. F. *J. Phys. Chem.* **1975**, *79*, 1855.

(27) (a) Geoffroy, M.; Rao, G.; Tancic, Z.; Bernardinelli, G. *J. Am. Chem. Soc*. **1990**, *112*, 2826. (b) Geoffroy, M.; Jouaiti, A.; Terron, G.; Cattani-Lorente, M.; Ellinger, Y. *J. Phys. Chem*. **1992**, *96*, 8241.

(28) (a) Hamerlinck, J. H. H.; Schipper, P.; Buck, H. M. *J. Am. Chem. Soc*. **1980**, *102*, 5679. (b) Hamerlinck, J. H. H.; Schipper, P.; Buck, H. M. *J. Am. Chem. Soc*. **1983**, *105*, 385.

(29) (a) Janssen, R. A. J.; Buck, H. M. *Chem. Phys. Lett*. **1986**, *132*, 459. (b) Janssen, R. A. J.; Sonnemans, M. H. W.; Buck, H. M. *J. Chem. Phys*. **1986**, *84*, 3694. (c) Janssen, R. A. J.; Sonnemans, M. H. W.; Buck, H. M. *J. Am. Chem. Soc*. **1986**, *108*, 6145. (d) Janssen, R. A. J.; Kingma, J. A. J. A.; Buck, H. M. *J. Am. Chem. Soc*. **1988**, *110*, 3018. (e) Janssen, R. A. J.; van der Woerd, M. J.; Aagaard, O. M.; Buck, H. M. *J. Am. Chem. Soc*. **1988**, *110*, 6001.

(30) Krusic, P. J.; Mahler, W.; Kochi, J. K. *J. Am. Chem. Soc*. **1972**, *94*, 6033.

(31) Schipper, P.; Jansen, E. H. J. M.; Buck, H. M. *Top. Phosphorus Chem*. **1977**, *9*, 407.

(32) Symons, M. C. R.; Petersen, R. L. *J. Chem. Soc., Faraday Trans. 2* **1979**, *75*, 210.

(33) Mattar, S. B. *Chem. Phys. Lett*. **1999**, *300*, 545.

(34) (a) Rega, N.; Cossi, M.; Barone, V. *J. Chem. Phys.* **1996**, *105*, 11060 (b) Barone, V. *J. Phys. Chem.* **1995**, *99*, 11659.

(35) Merritt, M. V.; Fessenden, R. W. *J. Chem. Phys.* **1972**, *56*, 2353.

(36) Hesse, C.; Leray, N.; Roncin, J. *J. Chem. Phys*. **1972**, *57*, 749.

(37) Sharp, J. H. S.; Symons, M. C. R. *J. Chem. Soc. A* **1970**, 3084.

(38) Krusic, P. J.; Kochi, J. K. *J. Am. Chem. Soc*. **1969**, *91*, 3938.

(39) Bennett, S. W.; Eaborn, C.; Hudson, A.; Jackson, R. A.; Root, K. D. J. *J. Chem. Soc. A* **1970**, 348.

(40) Cooper, J.; Hudson, A.; Jackson, R. A. *Mol. Phys*. **1972**, *23*, 209.

(41) Johnson, K. M.; Roberts, B. P. *J. Chem. Soc., Perkin Trans. 2* **1989**, 1111.

(42) Gerson, F.; Heinzer, J.; Bock, H.; Alt, H.; Seidl, H. *Helv. Chim. Acta* **1968**, *51*, 707.

(43) Gerson, F.; Krynitz, U.; Bock, H. *Helv. Chim. Acta* **1969**, *52*, 2512.

(44) Krynitz, U.; Gerson, F.; Wiberg, N.; Veith, M. *Angew. Chem., Int. Ed. Engl*. **1969**, *8*, 755.

(45) Alt, H.; Bock, H.; Gerson, F.; Heinzer, J. *Angew. Chem., Int. Ed. Engl*. **1967**, *6*, 941.

(46) Gerson, F.; Krynitz, U.; Bock, H. *Angew. Chem., Int. Ed. Engl*. **1969**, *8*, 767.

(47) Chatgilialoglu, C. *Chem. Rev*. **1995**, *95*, 1229.

(48) Chatgilialoglu, C.; Rossini, S. *Bull. Soc. Chim. Fr*. **1988**, 298.

(49) Bock, H.; Kaim, W. *J. Am. Chem Soc*. **1980**, *102*, 4429.

(50) Dunning, T. H.; Hay, P. J. In *Modern Theoretical Chemistry*; Schaeffer, H. F., III, Ed.; Plenum Press: New York, 1976; Vol. 3.

(51) Krishnan, R.; Binkley, J. S.; Seeger, R.; Pople, J. A. *J. Chem. Phys*. **1980**, *72*, 650.

(52) McLean, A. D.; Chandler, G. S. *J. Chem. Phys*. **1980**, *72*, 5639.

(53) Frisch, M. J.; Pople, J. A.; Binkley, J. S. *J. Chem. Phys*. **1984**, *80*, 3265.

(54) Guerra, M. *J. Chem. Soc., Perkin Trans. 2* **1995**, 1817.

(55) Davies, P. B.; Russell, D. K.; Thrush, B. A. *Chem. Phys. Lett*. **1979**, *44*, 421.

(56) Nelson, W.; Jackel, G.; Gordy, W. *J. Chem. Phys*. **1970**, *52*, 4572.

(57) Bonazzola, L.; Michaut, J. P.; Roncin, J. *J. Chem. Phys*. **1981**, *75*, 4829.

(58) Colussi, A. J.; Morton, J. R.; Preston, K. F. *J. Chem. Phys*. **1975**, *62*, 2004.

(59) Mishra, S. P.; Symons, M. C. R. *J. Chem. Soc., Dalton Trans*. **1976**, 139.

(60) Picone, R. F.; Raynor, J. B.; Ward, T. C. *J. Chem. Soc., Dalton Trans*. **1977**, 392.

(61) Begum, A.; Subramanian, S.; Symons, M. C. R. *J. Chem. Soc. A* **1970**, 1323.

(62) Boate, A. R.; Colussi, A. J.; Morton, J. R.; Preston, K. F. *Chem. Phys. Lett*. **1976**, *37*, 135.

(63) Begum, A.; Symons, M. C. R. *J. Chem. Soc., Faraday Trans*. **1973**, *69*, 43.

(64) Gerson, F.; Plattner, G.; Ashe, A. J., III; Maerkl, G. *Mol. Phys.* **1974**, *28*, 601.

(65) Nishikida, K.; Williams, F. *J. Am. Chem. Soc*. **1975**, *97*, 5462.

(66) Jongsma, C.; de Graaf, H. G.; Bickelhaupt, B. *Tetrahedron Lett*. **1974**, 1267.

(67) Fullam, B. W.; Mishra, S. P.; Symons, M. C. R. *J. Chem. Soc., Dalton Trans*. **1974**, 2145.

(68) Roberts, B. P.; Singh, K. *J. Organomet. Chem*. **1978**, *159*, 31.

(69) •Iwaizumi, M.; Kishi, T.; Watari, F.; Isobe, T. *Bull. Chem. Soc. Jpn.* **1975**, *48*, 3483.

(70) Davies, A. G.; Parrot, M. J.; Roberts, B. P. *J. Chem. Soc., Chem. Commun.* **1974**, 973.

(71) Gerson, F.; Merstetter, P.; Pfenninger, S.; Maerkl, G. *Magn. Reson. Chem*. **1997**, *35*, 384.

(72) Nishikida, K.; Williams, F. *J. Am. Chem. Soc*. **1974**, *96*, 4781.

(73) Christe, K. O.; Dixon, D. A.; Goldberg, I. B.; Schack, C. J.; Walther, B. W.; Wang, J. T.; Williams, F. *J. Am. Chem. Soc*. **1993**, *115*, 1129.

(74) Preston, K. F.; Sandall, J. P. B.; Sutcliffe, L. H. *Magn. Reson. Chem*. **1988**, *26*, 755.

(75) Wolmershauser, G.; Johann, R. *Angew. Chem., Int. Ed. Engl*. **1989**, *28*, 920.

(76) Wolmershauser, G.; Kraft, G. *Chem. Ber*. **1990**, *123*, 881.

(77) Windle, J. J.; Wiersema, A. K. *J. Chem. Phys*. **1963**, *39*, 1139.

(78) Sullivan, P. D. *J. Am. Chem. Soc.* **1968**, *90*, 3618.

(79) Geoffroy, M.; Lucken, E. A. C. *J. Chem. Phys*. **1971**, *55*, 2719.

(80) Davies, A. G.; Roberts, B. P.; Sanderson, B. R. *J. Chem. Soc., Perkin Trans. 2* **1973**, 626.

(81) Cavara, L.; Gerson, F.; Cowan, D. O.; Lerstrup, K. *Helv. Chim. Acta* **1986**, *69*, 141.

(82) Bock, H.; Roth, B.; Lakshikanthan, M. V.; Cava, M. P. *Phosphorus Sulfur Relat. Elem.* **1984**, *21*, 67.

(83) Gerson, F.; Wydler, C.; Kluge, F. *J. Magn. Reson*. **1977**, *26*, 271.

(84) Bramwell, F. B.; Haddon, R. C.; Wudl, F.; Kaplan, M. L.; Marshall, J. H. *J. Am. Chem. Soc.* **1978**, *100*, 4612.

(85) Gerson, F.; Gescheidt, G.; Knöbel, J.; Murata, I.; Nakasuji, K. *Helv. Chim. Acta* **1987**, *70*, 2065.

(86) Bryce, M. R.; Lay, A. K.; Chesney, A.; Batsanov, A. S.; Howard, J. A. K.; Buser, U.; Gerson, F.; Merstetter, P. *J. Chem. Soc., Perkin Trans 2* **1999**, 755.

(87) Perkins, C. W.; Clakson, R. B.; Martin, J. C. *J. Am. Chem. Soc*. **1986**, *108*, 3206.

(88) Rundel, W.; Scheffler, K. *Angew. Chem., Int. Ed. Engl*. **1965**, *4*, 220.